Determination of the Intracellular Concentrations of Metabolites in *Escherichia coli* Collected during the Exponential and Stationary Growth Phases using Liquid Chromatography-Mass Spectrometry

Changhun Park, Changhun Park,[†,‡] Youn-jin Lee,[†] Sang Yup Lee,[§] Han Bin Oh,[†,*] and Jinwon Lee[*]

Department of Chemical and Biomolecular Engineering, Sogang University, Seoul 121-742, Korea
[*]E-mail: jinwonlee@sogang.ac.kr
[†]Department of Chemistry, Sogang University, Seoul 121-742, Korea. [*]E-mail: hanbinoh@sogang.ac.kr
[‡]Clinical Trials Center, Yonsei University Health System, Seoul 120-725, Korea
[§]Department of Chemical and Biomolecular Engineering, Korea Advanced Institute of Science and Technology,
Daejeon 305-701, Korea
Received September 30, 2010, Accepted December 3, 2010

In the present study, we demonstrate that SRM LC-MS/MS method developed by Luo *et al.* (ref. 10) can be successfully applied to the quantitative analysis of intracellular metabolites in *E. coli* that are collected at the exponential and stationary growth phases. A focus is given on measuring the changes in the concentrations of intracellular metabolites in batch cultures, which were induced during both the dynamically changing exponential and stationary growth phases. The following intracellular metabolites are quantified in the exponential and stationary phases of *E. coli* growth, using the SRM mode of a triple quadrupole mass spectrometer: glucose-1-phosphate, fructose-1,6-bisphosphate, phosphoenolpyruvate, pyruvate, acetyl-coenzyme A, 6-phosphogluconate, ribulose-5-phosphate, xylulose-5-phosphate, erythrose-4-phosphate. The determined intracellular metabolite concentration profiles are shown to be in a good agreement with the growth profiles of *E. coli*, which clearly indicates that SRM LC-MS/MS can be successfully used for following the metabolite changes induced at different growth stages.

Key Words: Metabolomics, SRM, *E. Coli*, LC-MS, Metabolites

Introduction

Metabolomics, a comprehensive, quantitative analysis of metabolites in a biological system, has greatly enhanced the understanding of biological phenomena and systems.[1-4] Along with other -omics technologies such as genomics, transcriptomics, and proteomics, metabolomic investigations have increased integrative knowledge of biochemical and biological mechanism in complex systems.[5] Since metabolomics represents the endpoint of the -omics cascade, it is the closest to phenotype, and its application is now rapidly expanding.[5,6]

In recent years, studies of cellular systems have become increasingly active and productive, due to the recent advance in the optimization of both cellular growth and the production process. Cellular growth is primarily enhanced by metabolic engineering, and improvements in productivity are primarily accomplished through the advancements in bioprocess engineering.[7] To enhance cellular growth, understanding of the central carbon metabolism (e.g., glycolysis, the pentose phosphate pathway, and the TCA cycle) is crucial because these pathways are closely involved in biosynthetic reactions, energy metabolism, and anaplerotic reactions.[7] The understanding of the central carbon metabolism, for example, of *E. coli*, and its related *in vivo* kinetics can provide us with a framework with which a stream of modifications of intermediary metabolisms can be made to increase the biosynthetic production of primary and secondary metabolites.[7]

A detailed understanding of the central carbon metabolism can be achieved through the quantification of the metabolites involved in their pathways. Measurements of metabolite concentrations provide quantitative information concerning the kinetics of metabolism; these measurements can be used for mathematical modeling. Mass spectrometry has emerged as a key technology for the quantitative analysis of metabolites.[7,8] Mass spectrometry is very useful for the analysis of extracellular and intracellular metabolites due to its extraordinary sensitivity, low sample consumption, and high selectivity. Gas chromatography-mass spectrometry (GC-MS) has been described as the gold standard for metabolomic research.[8] This tool is becoming increasingly popular due to its ability of chromatographic separation, analyte-specific detection, quantification, and identification of unknown metabolites.[5,8,9] However, this method requires additional chemical derivatization procedures to reduce the polarity and to increase the volatility and thermal stability of the metabolites under examination.

In contrast, electrospray ionization mass spectrometry (ESI-MS) has many advantages over GC-MS because ESI-MS does not require the chemical derivatization of samples. Furthermore, when coupled with chromatography, this method can provide additional dimensionality. Chromatographic separation even makes it possible to distinguish isomers, which produce very distinctive MS/MS patterns.[10]

The most difficult types of metabolites to analyze are high polarity metabolites, such as nucleotides and sugar phosphates, due to their highly ionic nature.[11] To analyze these types of metabolites, anion exchange chromatography and ion pairing chromatography-mass spectrometry are reported to be useful.[10-14] Most recently, Luo *et al.* developed a highly selective and sensitive ion pairing-liquid chromatography-mass spectrometry method for the simultaneous identification and quantification
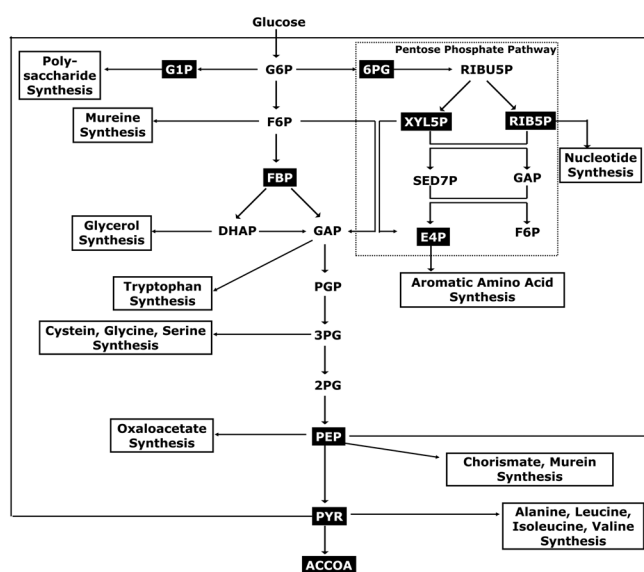
Scheme 1. Glycolysis metabolic pathway and pentose phosphate pathway in *E. coli*; metabolites examined in the present study are denoted in filled boxes

of 29 negatively charged compounds including sugar phosphates, nucleotides, and carboxylic acids by using a C18 reversed-phase column.[10] They employed tributylammonium acetate as the volatile ion pair modifier, resulting in low limits-of-detection (LOD).

In the present study, we demonstrate that the above-mentioned method developed by Luo *et al.* can be successfully applied to the quantitative analysis of intracellular metabolites in *E. coli*, which are collected at the exponential and stationary phases of growth.[10] Examination of the metabolite concentration profile changes at different growth phases is an interesting subject in metabolomics. More specifically, measurements of intracellular metabolites at various growth stages are crucial for the development of mathematical models. This kinetic modeling is currently underway and will be presented in a forthcoming paper. In this study, measurements were made for the following selected metabolites that are involved in the central carbon metabolism; G1P (Glucose-1-phosphate), FBP (Fructose-1,6-bisphosphate), PEP (Phosphoenolpyruvate), PYR (Pyruvate), AcCoA (Acetyl-coenzyme A), 6PG (6-Phosphogluconate), Ri5P (Ribulose-5-phosphate), X5P (Xylulose-5-phosphate), and E4P(Erythrose-4-phosphate). These metabolites are key intermediates in glycolysis metabolic pathway and pentose phosphate pathway (refer to Scheme 1).[15]

Materials and Methods

Chemicals. *E. coli* K-12 strain W3110 (KCTC 2223) was obtained from the BRC (Biological resource center in Korea). Extracellular and intracellular metabolite standards were purchased from Sigma and Fluka. High purity solvents and reagents were used to avoid the appearance of interfering MS peaks and high background. Tributylamine was obtained from Aldrich and acetic acid (GC standard grade) was purchased from Fluka. The solvents used for chromatography were of HPLC grade.

Culture Condition. Precultivation was performed overnight (12 h, 200 rpm, 37 ^{o}C) in a shake flask (500 mL) containing 200 mL of precultivation medium (LB medium). *E. coli* K-12 strain W3110 was batch cultivated in a stirred bioreactor (150 rpm) with a working volume of 2.0 L at 37 ^{o}C. Synthetic mineral medium was used for the batch culture. The concentrations of components in the synthetic mineral medium included: 4.0 g/L Na_2SO_4; 5.36 g/L $(NH_4)_2SO_4$; 1.0 g/L NH_4Cl; 7.3 g/L K_2HPO_4; 1.8 g/L NaH_2PO_4 H_2O; 12.0 g/L $(NH_4)_2$-H-citrate; 4.0 mL/L $MgSO_4$ (1 M); 6.0 mL/L trace element solution; 0.02 g/L thiamine; and 20.0 g/L glucose. The air flow was kept constant at 2 L/min and the pH was controlled at 7.0 by the addition of 2 M NaOH. To prevent foam formation, an anti-foam agent was added periodically.

Sampling, Quenching, and Extraction. Samples were taken every 2 h after batch culture initiation. The culture sample vials (5 mL) were plunged rapidly into an equal volume of 60% aqueous methanol ($-$40 ^{o}C). The quenched biomass was centrifuged for 8.5 min (i.e., the minimum time period required to form a pellet) at 3,000 $\times$ g and $-$9 ^{o}C. The supernatant was removed rapidly, and an aliquot (1 mL) was retained to assess the leakage of internal metabolites. The pellets and supernatants were frozen in liquid nitrogen and stored at $-$80 ^{o}C for further analysis.[16] The first step of the methanol extraction method froze the pellets. The biomass pellets were suspended in 500 µL of 100% methanol ($-$40 ^{o}C) and frozen in liquid nitrogen. The second step was thawing. The biomass pellets were allowed to thaw on dry ice. The freeze-thaw rotation was performed three times to cause the metabolites to leak from the cells. The suspensions were then centrifuged at 16,000 $\times$ g at $-$9 ^{o}C for 5 min. The supernatant was retained and stored on dry ice, and a 500 µL aliquot of 100% methanol ($-$48 ^{o}C) was then added to the pellet. The above procedure was repeated, and the two aliquots were combined. The sample was stored at $-$80 ^{o}C.[17]

Measurement of Extracellular Metabolites Concentration. The concentrations of glucose, lactate, formate and acetate were analyzed using a high-performance liquid chromatography (HPLC, UV 730D detector, RI 750F monitor; Younglin, Korea) equipped with an ion-exchange column (Aminex HPX-87H, 300 mm $\times$ 7.8 mm; Bio-Rad) using 0.005 N H_2SO_4 as the mobile phase at 55 ^{o}C and a flow rate of 0.6 mL/min.

LC-MS/MS Measurement. All LC-MS/MS experiments were carried out using an Applied Biosystems/MDS Sciex API 3200 triple quadrupole mass spectrometer (AB/MDS Sciex, Concord, Canada) equipped with a turbo-ion spray source. The mass spectrometer was coupled with an Agilent 1200 series HPLC system (Agilent Technologies, Santa Clara CA, USA). Data were acquired and processed using Analyst software (version 1.4.2, AB/MDS Sciex, Concord, Canada). The mass spectrometer was operated in the negative ion and selected reaction monitoring (SRM) modes. The declustering potential (DP), collision energy (CE) and collision cell exit potential (CXP) were carefully optimized. The entrance potential (EP) was fixed at $-$10 V throughout all experiments. The MS parameters were as follow: the ionspray voltage was $-$4,500 V, the nebulizer gas (GS1), auxiliary gas (GS2), curtain gas (CUR) and collision gas (CAD) values were 20, 20, 10, and 5 (arbitrary units), respectively. The auxiliary gas temperature was maintained at 500 ^{o}C. The chro-

Table 1. Gradient profile used in the LC-MS/MS method

| Step	Total time (min)	Eluent A (vol %)	Eluent B (vol %)
1	15.00	100.0	0.0
2	25.00	80.0	20.0
3	55.00	80.0	20.0
4	60.00	65.0	35.0
5	65.00	65.0	35.0
6	70.00	40.0	60.0
7	75.00	40.0	60.0
8	75.10	10.0	90.0
9	80.00	10.0	90.0
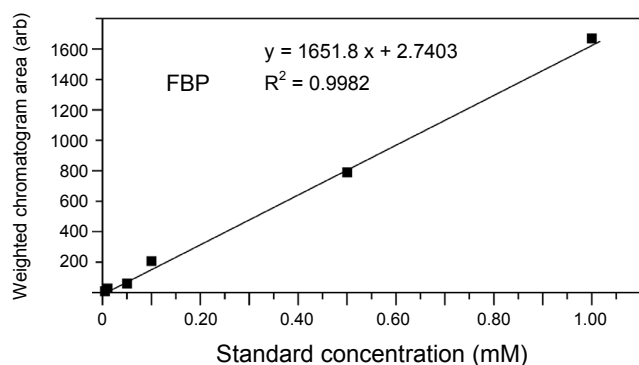
Figure 1. The weighted calibration curve obtained for FBP.

matographic separation was achieved with a Synergi Hydro-RP (C18) 150 mm × 2.1 mm I.D., 4 μm 80 Å particles column (Phenomenex, Torrance, CA, USA) at room temperature. Eluent A was a 10 mM aqueous tributylamine solution with its pH adjusted to pH 4.95 using 15 mM acetic acid, and eluent B was methanol. A binary gradient at the flow rate of 0.2 mL/min is shown in Table 1.

Quantification. Quantitative analysis was made using 'weighted' regression analysis method.[18] Primary stock aqueous solutions were prepared at a concentration of 5mM for each metabolite. From this solution one stock solution of 100 μM standard mixture was prepared in water. Aliquots of this standard mixture were used for calibration and for the quality control (QC) standards. The calibration curve was obtained by analyzing standard solutions at six concentrations, ranging from 0.005 mM to 1 mM (0.005, 0.01, 0.05, 0.1, 0.5, and 1 mM). The calibration curves were constructed by plotting the SRM chromatogram area of the compound (weighted to $1/x$, where x is the concentration in mM) against the concentration of the compound (x). For example, Figure 1 shows the weighted calibration curve obtained for FBP. Weighted linear regression was used to fit the calibration curve and the linearity for each compound was evaluated using the calibration curve.

Results and Discussion

Growth Profile of the Batch Culture. The growth profile of the *E. coli* batch culture was obtained at 2 hour intervals for up to 18 hours by measuring the dry weights of the biomass and the concentrations of the extracellular metabolites (see Figure 2). The dry weights of the biomass (in g/L) were determined by
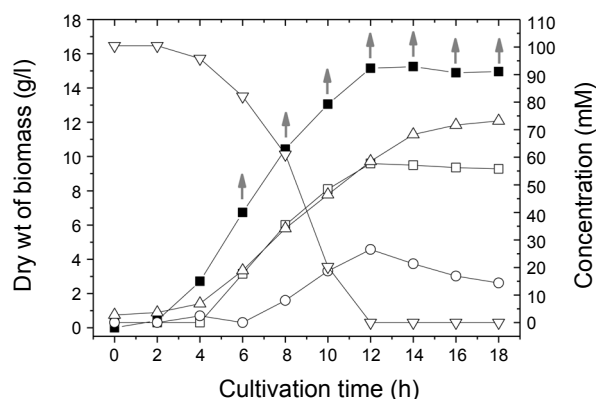
Figure 2. Growth profiles of bioreactor batch cultures: (■) Dry weight of the biomass. The upward arrow indicates the time at which samples were taken for intracellular metabolite analyses. Extracellular metabolite concentration profile: (▽) Glucose, (△) Acetate, (□) Formate, and (○) Lactate.

measuring the optical transmittance of the collected culture media at 600 nm; these values are denoted as solid squares in Figure 2. The concentrations of the four extracellular metabolites, glucose (▽), acetate (△), formate (□), and lactate (○), which will be determined using SRM quantitative analysis, are also shown in Figure 2. These dry weights indicate that the *E. coli* grew exponentially for up to 12 hours before reaching the stationary phase. Similar production profiles were seen for "growth-associated" products,[19] *i.e.*, acetate, formate, and lactate. After ~12 h, the "growth-associated" metabolites showed a short period of arithmetic growth before the cells entered the stationary phase. Interestingly, the end of the exponential phase coincided with the almost complete consumption of glucose in the extracellular medium by *E. coli*.

Quantitative Analysis of Intracellular Metabolites. For quantitative analysis of intracellular metabolites, the MS and MS/MS experimental parameters were optimized for the standard metabolite samples using directly infused electrospray ionization mass spectrometry (ESI-MS); the standard samples examined in this study included G1P (Glucose-1-phosphate), FBP (Fructose-1,6-bisphosphate), PEP (Phosphoenolpyruvate), PYR (Pyruvate), AcCoA (Acetyl-coenzyme A), 6PG (6-Phosphogluconate), Ri5P (Ribulose-5-phosphate), X5P (Xylulose-5-phosphate), and E4P (Erythrose-4-phosphate). The detection of the metabolites was made using the negative-ion mode because all of the metabolites of interest have low pK_a values. All of the metabolites examined in this study have a phosphate group in common, except for PYR, and thus their collision induced dissociation (CID) MS/MS spectra shared similar fragmentation characteristics.

Mass Spectrometric Analysis. As shown in Figure 3, $[PO_3]^-$ or $[H_2PO_4]^-$ was a dominant CID MS/MS metabolic product, except when PYR were analyzed. For PYR, decarboxylated precursor ions were found at *m/z* 43. It is important to note that Ri5P and X5P are isobaric compounds (detected at *m/z* 229) differing only in the stereochemistry at C3. They are indistinguishable by MS/MS due to their structural similarities. These observations are summarized in Table 2, where the *m/z* values of metabolites of interest, [M-H]⁻, and their main product ions
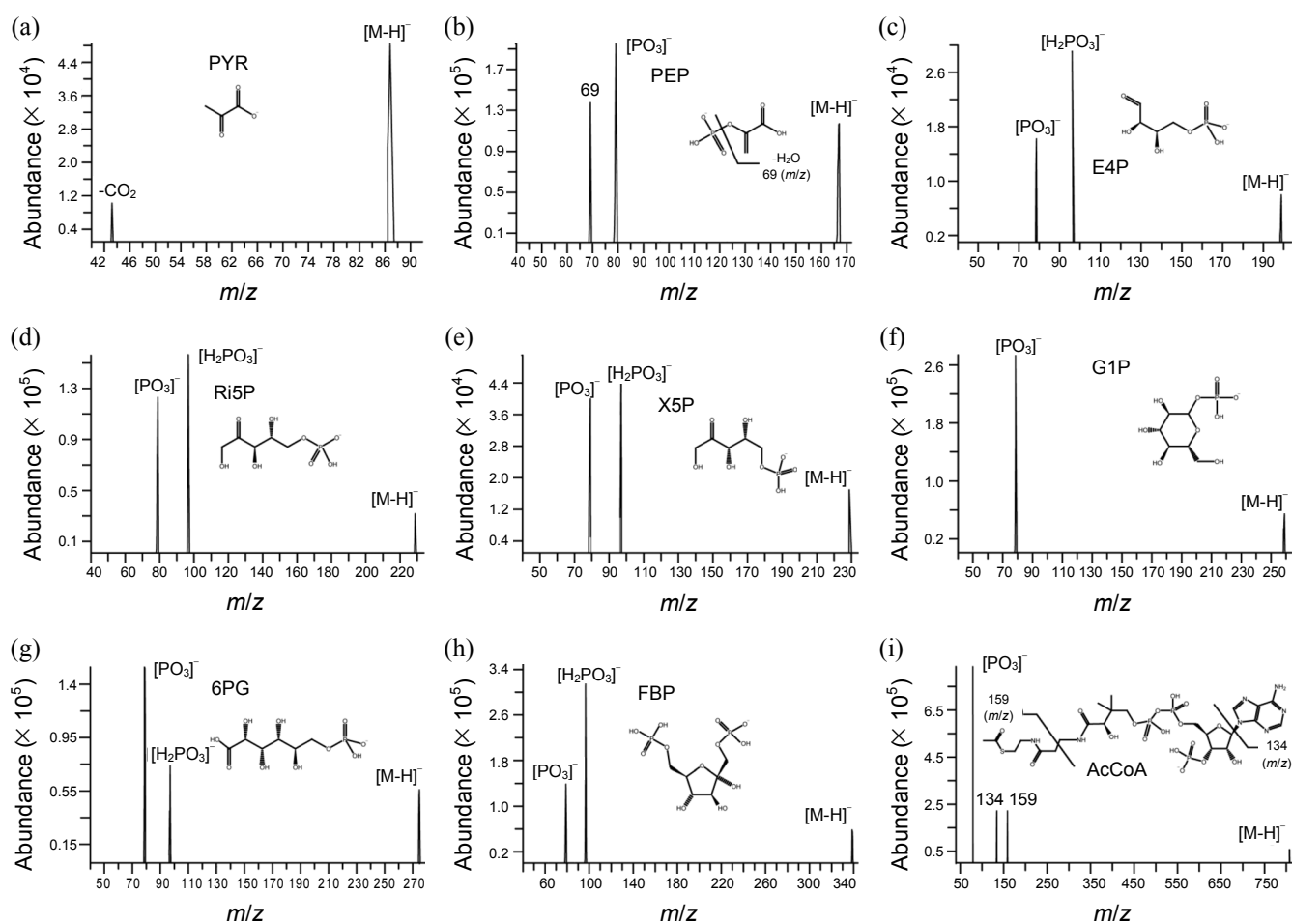
Figure 3. Collision induced dissociation (CID) product mass spectrometry spectrum: (a) PYR standard; (b) PEP standard; (c) E4P standard; (d) Ri5P standard; (e) X5P standard; (f) G1P standard; (g) 6PG standard; (h) FBP standard; and (i) AcCoA standard.

are indicated. The experimental parameters for mass spectrometry are also indicated in the table. The main products shown in Table 2 were used as the SRM transitions in the mass spectrometric quantifications.

The metabolites were quantified using a triple-quadrupole mass spectrometer in the SRM mode. The liquid chromatography parameters used in this study, such as the gradient profile and ion-pairing reagents, were the same as those used by Luo *et al.*[10] These authors found that tributylamine (TBA) was an optimal ion-pairing agent in terms of separation resolution and retention time, compared to other trialkylamines. Furthermore, they found that pH was also crucial for optimal chromatographic peak resolution; pH value of 4.95 was shown to be best. Therefore, a 10 mM aqueous TBA solution adjusted to pH 4.95 was used in this study (see Materials and Methods).

Chromatographic Analysis. Figure 4 shows selected ion chromatograms (SICs) for the nine metabolites that were obtained from the standard mixture. It was crucial to obtain retention times for the sample metabolites. Knowledge of both the specific SRM transition and the retention time is required for quantitative metabolite analysis because it can minimize the chance of producing a false positive reading. The elution order shown in Figure 4 is consistent with that of Luo *et al.*, although there were some differences in specific retention times.[10] The reten-

tion time for each metabolite was used for further analysis of the intracellular metabolites.

The limits of detection (LOD) were also determined for the metabolites by taking three times the standard deviation of the background signals. The obtained LODs ranged from 0.01 to 0.24 μM, except for 2.27 μM for PYR (see Table 3). For PYR, the relatively poor product ion signal at *m/z* 43 limited the LODs; these results are in agreement with those of Luo *et al.*[10] The LODs obtained in this study were approximately one order of magnitude higher than those of Luo *et al.*,[10] but they were approximately the same order of magnitude as those obtained in other studies.[12,14,20] The higher LODs were presumably due to the use of a less sensitive mass spectrometer (Applied Biosystems/MDS Sciex API 3200 triple quadrupole mass spectrometer versus 4000 Q TRAP triple quadrupole mass spectrometer). Furthermore, our sample injection volume was rather small, *i.e.*, 1 μL.

Intracellular Metabolite Concentration Profiles at Two Different Growth Phases. The concentrations of intracellular metabolites at various *E. coli* growth phases were determined using the weighted regression analysis method described in the experimental section.[18] The *E. coli* growth phase, which is reflected in the dry weight of the biomass, is indicated by solid squares in Figure 2. For intracellular metabolite analyses, 5 mL sam-
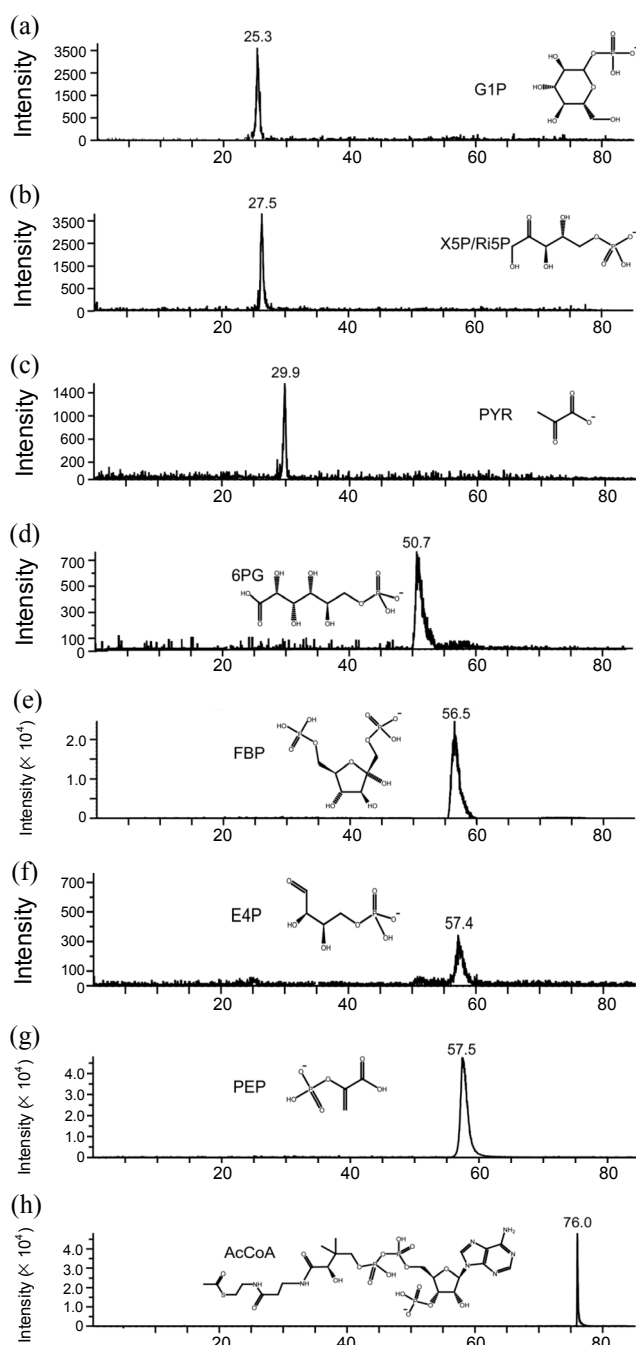
Figure 4. Single reaction monitoring (SRM) chromatogram for selective ion chromatogram: (a) G1P; (b) X5P/Ri5P; (c) PYR; (d) 6PG; (e) FBP; (f) E4P; (g) PEP; and (h) AcCoA. The concentrations of standard metabolites were as follow: G1P, 0.11 mg/mL; X5P/Ri5P, 0.001 mg/mL; PYR, 0.061 mg/mL; 6PG, 0.11 mg/mL; FBP, 3.77 mg/mL; E4P, 0.22 mg/mL; PEP, 1.67 mg/mL; AcCoA, 0.89 mg/mL.

Table 2. Metabolite ions monitored in the LC-MS/MS experiments: nominal *m/z* values of precursor ions, [M-H]⁻; nominal *m/z* values of main product ions; mass spectrometry experimental parameters. DP: declustering potential, CE: collision energy, CXP: collision cell exit potential

Metabolite	[M-H]⁻ (*m/z*)	Main product ion (*m/z*)	DP (V)	CE (V)	CXP (V)
PYR	87	43, -CO_2	−20	−10	−6
PEP	167	79, -H_3PO_4	−50	−50	−6
E4P	199	97, $[H_2PO_4]^-$	−45	−14	−6
Ri5P	229	97, $[H_2PO_4]^-$	−20	−16	−6
X5P	229	97, $[H_2PO_4]^-$	−20	−16	−6
G1P	259	97, $[H_2PO_4]^-$	−35	−18	−6
6PG	275	79, $[PO_3]^-$	−30	−50	−6
FBP	339	97, $[H_2PO_4]^-$	−27	−30	−6
AcCoA	808	79, $[PO_3]^-$	−115	−96	−6

Table 3. Limit of detection: LOD, intracellular LOD, and absolute quantities [ng/mL] in cell extracts

Compound	LOD (µM)	Intracellular LOD (µM)	LOD (ng/mL)
G1P	0.08 µM	2.84 µM	20 ng/mL
FBP	0.17 µM	0.182 µM	0.058 ng/mL
PEP	0.1 µM	5.47 µM	0.017 ng/mL
PYR	2.27 µM	21.46 µM	200 ng/mL
AcCoA	0.08 µM	0.311 µM	0.065 ng/mL
6PG	0.24 µM	9.27 µM	67 ng/mL
R5P/ X5P	0.02 µM	0.022 µM	4 ng/mL
E4P	0.01 µM	0.039 µM	2 ng/mL

the intracellular volume of *E. coli*, a correction was again made for these values to account for the varying biomass dry weights of the samples at given times (refer to Figure 2); these results are shown in Figure 5. For the correction, the value of 2.15 mL/g dry cell mass was used for the intracellular volume of the *E. coli* cells.[21] This procedure was repeated three times to obtain the average concentration of the metabolites.

Figure 5 shows the average intracellular concentration of metabolites in *E. coli* taken at the seven different cultivation times. Each metabolite shows quite a different concentration profile. For example, G1P, FBP, and 6PG declined fairly steadily, while PEP, PYR, AcCoA, X5P+Ri5P, and E4P showed a trend of an increase at early cultivation times, followed by a decrease, or vice versa. A distinctive range of concentrations was exhibited for each metabolite. The two extreme cases were PYR and X5P + Ri5P, which were on the order of 1 and 0.001 mM, respectively. Specifically, G1P and 6PG had very similar concentration ranges, which spanned from 0 to 0.8 mM. For FBP, AcCoA, and PEP, the concentrations were much lower than those of G1P and 6PG. In contrast, PYR showed much higher concentrations (0 - 8.65 mM). X5P/Ri5P and E4P exhibited significantly lower concentrations, which were in the range of 0 to 0.0031 mM.

To better understand the metabolic changes that occurred around 12 h after the initiation of batch cultivation, the concentrations of intracellular metabolites were compared to the specific growth rates of *E. coli* in the batch culture (Table 4). The
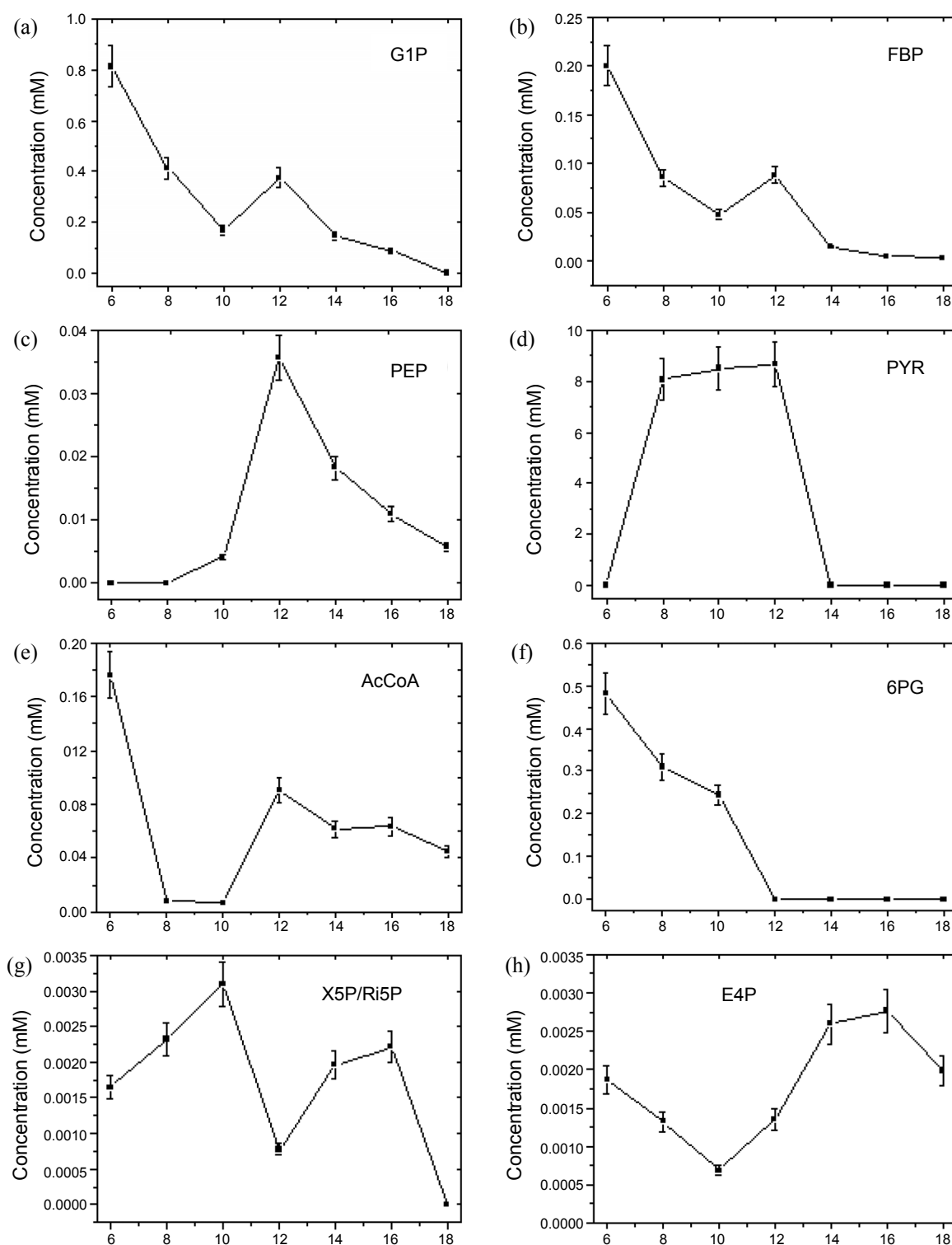
ples of the batch culture taken at 6, 8, 10, 12, 14, 16, and 18 hours are denoted by upward arrows in Figure 2. The concentrations for the nine intracellular metabolites determined by the weighted regression analysis method for the given sample volume were as follow: G1P, 0 - 122.2 µM; FBP, 13.3 - 29.0 µM; PEP, 1.18 - 11.6 µM; PYR, 0 - 29.6 µM; AcCoA, 1.87 - 29.6 µM; 6PG, 0 - 69.9 µM; X5P/Ri5P, 0.24 - 0.87 µM; E4P, 0.193 - 0.885 µM. To obtain the intracellular metabolite concentrations within

Figure 5. Cultivation time profiles of intracellular metabolite concentrations (in the intracellular volume of *E. coli*): (a) G1P; (b) FBP; (c) PEP; (d) PYR; (e) AcCoA; (f) 6PG; (g) X5P/Ri5P; and (h) E4P. The procedure was repeated three times to obtain the average concentration of the metabolites.

specific growth rates of the *E. coli* batch culture and the concentrations of individual intracellular metabolite were determined from Figure 2. The specific growth rate of 0.0318 h^{-1} occurred at 12 h. Most intracellular metabolite concentrations decreased in the range of specific growth rates from 0.0043 - 0.0318 h^{-1},

except those of E4P and X5P/Ri5P. The concentrations of E4P and X5P/Ri5P increased in the range of specific growth rates from 0.0043 - 0.0318 h^{-1}. The specific growth rate of 0.0043 h^{-1} occurred 16 h after the initiation of the batch culture.

Analysis of Metabolites in Two Different Growth Phases.

Table 4. Relationship between the intracellular metabolite concentration and the specific growth rate of *E. coli*

Specific growth rate (h^{-1})	G1P (mM)	FBP (mM)	PEP (mM)	PYR (mM)	AcCoA (mM)	6PG (mM)	X5P + Ri5P (mM)	E4P (mM)
−0.0704	0	0.0028	0.0057	0	0.0451	0	0	0.0019
0.0043	0.0886	0.0047	0.0109	0	0.0634	0	0.0022	0.0028
0.0258	0.1468	0.0143	0.0183	0	0.0619	0	0.0019	0.0026
0.0318	0.3751	0.0880	0.0356	8.658	0.0908	0	0.0008	0.0014
0.0603	0.1680	0.0474	0.0042	8.490	0.0071	0.2439	0.0031	0.0007
0.1490	0.4130	0.0852	0	8.050	0.0083	0.3099	0.0023	0.0013
0.3359	0.8121	0.2002	0	0	0.1760	0.4826	0.0016	0.0019

The concentration profiles of the intracellular metabolites in this study can be related to a few metabolic pathways such as the Embden-Meyerhof pathway and the pentose phosphate pathway. The metabolites involved in the Embden-Meyerhof pathway, *e.g.*, PEP, FBP, PYR, generally showed a remarkably different concentration profile from those involved in the pentose phosphate pathway (X5P/Ri5P, E4P). In particular, in the stationary phase, metabolites in the Embden-Meyerhof pathway exhibited a continuous decrease in concentration, while metabolites in the pentose phosphate pathway exhibited a rapid increase during the 12 - 14 h period of the stationary phase (see Figure 5).

The concentration profiles of some intracellular metabolites can be understood in relation to the metabolic pathways for the metabolites of interest. For example, PYR showed a sharp drop in concentration after 12 h, due to the shortage of precursor metabolites, *e.g.*, PEP, which are necessary for the formation of PYR. In the case of X5P/Ri5P and E4P, which are precursors in the amino acid synthesis pathway, the concentration profiles show an accumulation of these metabolites at 12 - 16 h. This finding may be related to the previous observation that the protein synthesis pathway is inhibited at the early stage of the stationary phase of growth.[22] The inhibited amino acid synthesis pathway may lead to the accumulation of precursor metabolites.

The intracellular metabolite concentration profiles shown in Figure 5 generally coincide with those of extracellular metabolites in Figure 2. For example, the intracellular PYR concentration fell sharply after 12 h, which is consistent with the exhaustion of glucose (▽) at 12 h, that is, at the end of the exponential phase (see Figure 2). It was also found that AcCoA showed some residual concentrations even after 18 h in the stationary phase. This is consistent with the observation that the extracellular acetate concentrations showed a slow increase even in the stationary phase.

Conclusion

Metabolic regulation in the *E. coli* K12 strain W3110 was studied by monitoring changes in the intracellular metabolite concentrations at two different growth phases, stationary and exponential. An extraction procedure using 100% methanol (−40 $^{\circ}$C) was performed to extract intracellular metabolites from *E. coli*. All of the quantifications of intracellular metabolites were made using the SRM mode of triple-quadrupole mass spectrometer. This method allowed for the combined separation and quantification of intracellular metabolites from the most interesting biological compounds in central carbon metabolism.

This method can be successfully applied to identify and quantify these intracellular metabolites in various cell extract samples. The intracellular metabolite concentration data can be used to help understand of microbial metabolism. This can lead to mathematical modeling based on accurate intracellular metabolite concentration measurements of the most important reactants in microbial metabolism.

References

1. Fiehn, O. *Comparative and Functional Genomics* **2001**, *2*, 155.
2. Fiehn, O.; Kopka, J.; Dörmann, P.; Altmann T.; Trethewey, R. N.; Willmitzer, L. *Nature Biotechnol.* **2000**, *18*, 1157.
3. Gipson, G. T.; Tatsuoka, K. S.; Sokhansanj, B. A.; Ball, R. J.; Connor, S. C. *Metabolomics* **2008**, *4*, 94.
4. Hollywood, K.; Brison, D. R.; Goodacre, R. *Proteomics* **2006**, *6*, 4716.
5. Dettmer, K.; Aronov, P. A.; Hammock, B. D. *Mass Spectrometry Reviews* **2007**, *26*, 51.
6. Shulaev, V. *Briefings in Bioinformatics* **2006**, *7*, 128.
7. Buchholz, A.; Hurlebaus, J.; Wandrey, C.; Takors, R. *Biomolecular Engineering* **2002**, *19*, 5.
8. Dunn, W. B.; Ellis, D. I. *Trends in Analytical Chemistry* **2005**, *24*, 285.
9. Moco, S.; Bino, R. J.; De Vos, R. C. H.; Vervoort, J. *Trends in Analytical Chemistry* **2007**, *26*, 855.
10. Luo, B.; Groenke, K.; Takors, R.; Wandrey, C.; Oldiges, M. *Journal of Chromatography A* **2007**, *1147*, 153.
11. Coulier, L.; Bas, R.; Jespersen, S.; Verheij, E.; Van der werf, M. J.; Hankemeier, T. *Analytical Chemistry* **2006**, *78*, 6573.
12. Huck, J. H. J.; Struys, E. A.; Verhoeven, N. M.; Jakobs C.; Van der knap, M. S. *Clinical Chemistry* **2003**, *49*, 1375.
13. Sekiguchi, Y.; Mitsuhashi, N.; Kokaji, T.; Miyakoda, Hi.; Mimura, T. *Journal of Chromatography A* **2005**, *1085*, 131.
14. Van dam, J. C.; Eman, M. R.; Frank, J.; Lange, H. C.; Van dedem, G. W. K.; Heijnen S. J. *Anal. Chim. Acta* **2002**, *460*, 209.
15. Chassgnolie, C.; Noisommit-Rizzi, N.; Schmid, J. W.; Mauch, K.; Reuss, M. *Biotechnol. Bioeng.* **2002**, *79*, 53.
16. Winder, C. L.; Dunn, W. B.; Schuler, S.; Broadhurst, D.; Jarvis, R.; Stephens, G. M.; Goodacre, R. *Analytical Chemistry* **2008**, *80*, 2939.
17. Maharjan, R. P.; Ferenci, T. *Analytical Biochemistry* **2003**, *313*, 145.
18. Miller, J. C.; Miller, J. N. *Statistics for Analytical Chemistry*; Ellis Horwood Ltd.: Chichester, UK, 1988.
19. Rao, D. G. In *Introduction to Biochemical Engineering*; McGraw-Hill: New delhi, India, 2006; p169.
20. Soga, T.; Ueno, Y.; Naraoka, H.; Ohashi, Y.; Tomita, M.; Nishioka, T. *Analytical Chemistry* **2002**, *74*, 2233.
21. Pramanik, J.; Keasling, J. D. *Biotechnol Bioeng.* **1997**, *56*, 399
22. Kolter, R.; Siegele, D. A.; Torma, A. *Annual Reviews Microbiol.* **1993**, *47*, 855.